Indian Journal of Engineering & Materials Sciences
Vol. 29, October 2022, pp. 581-585
DOI: 10.56042/ijems.v29i5.52987

Effect of Thermal Strain, Induced by Cryogenic Cooling, on a High Homogeneity Superconducting Magnet for MRI Applications

Sankar Ram Thekkethil[a,b], Vikas Rastogi[a], & Soumen Kar[b]*
[a]Delhi Technological University, New Delhi, 110 042
[b]Inter-University Accelerator Centre, New Delhi, 110 067

Received: 28 July 2021; Accepted: 23 March 2022

The heart of the modern whole body MRI scanners is a superconducting magnet producing the required magnetic field with high homogeneity. The superconducting magnet operates at 4.2 K (-268.95 ^{o}C) and thus is kept dipped in liquid helium to maintain its superconducting state. This cool down of the multi-coil magnet from room temperature to the LHe temperature generates thermal strains in the magnet structure which deforms the magnet. These deformations are found to affect the final magnetic field homogeneity and introduce artifacts in the MR images. We report our results on studies on the stresses induced in the bobbin and the coils consequent upon cooling the magnet to 4.2 K. The maximum von Mises stress in the coils is calculated to be 31.3 MPa while in the bobbin it comes out to be 60 MPa. We find that the cool down causes a relative movement of the coils which in turn degrades the field homogeneity from 5.5 ppm to 278 ppm. The centre field is found to increase by 60 G is caused by a reduction in the overall cross-section of the coils. The change in homogeneity is also analysed in terms of Legendre polynomials where we found that the relative displacements of the coils introduce odd order terms to the polynomial expansion terms which were not present in the original design.

Keywords: Superconducting Magnets, Thermal Strain, Field homogeneity, Cryogenic cooling

1 Introduction

An MRI scanner with a 1.5 T or 3.0 T superconducting magnet has become an essential clinical diagnostic tools in a hospital. The superconducting magnet creates a highly homogenous magnetic field within a sphere of 45-50 cm diameter at the magnet centre, called the Field of View (FOV). Within this FOV, a field homogeneity of the order of 10 ppm is maintained to achieve quality images. To minimise the amount of superconductor and thus the cost, modern MRI magnets are built as an assembly of multiple axially symmetric solenoidal coils mounted on a rigid bobbin. Commercial MRI magnets, now a days, have anywhere between 6-12 discrete coils instead of a single long solenoid used in earlier designs. Modern MRI magnets are also actively shielded, where two or more shield coils, with current direction opposite to those of primary coils, are used to restrict the fringe fields outside the magnet.[1,2]

The most widely used superconductor for MRI magnets is copper stabilized Niobium-Titanium (Nb-Ti) conductor which has a critical temperature of 9 K. Therefore the magnet needs to be cooled well below 9 K to reach the superconducting state. The nearest cryogen available for this temperature regime is liquid helium, which has a boiling point of 4.2 K at atmospheric pressure. The cool down of the magnet from room temperature (~300 K) to cryogenic temperatures (4.2 K) generates thermal stresses in the coils and the bobbin. These stresses, if kept unchecked, can permanently damage the coils and also impact the current carrying capacity of the superconductor. Based on the materials used for construction, the cool down also creates differential contraction between the coils and bobbin causing unpredictable movement of coils during operation. The relative displacements during cool down and further movements during operation (due to the Lorentz force) can alter the magnetic coordinates thus destroying the indented design. Thus it is essential to study the thermal strains and their effect on the final magnet before taking up the fabrication of the magnet.

2 1.5 T MRI Magnet

We have designed a Nb-Ti based MRI magnet to generate a central field of 1.5 T with ±5 ppm homogeneity in a 45 cm Field of View (FOV).[3] The magnet has three pairs of primary coils and one pair of shield coil positioned symmetrically across the

Corresponding authors (E-mail: Kar.soumen@gmail.com

mid-plane. The final magnet will have a maximum diameter of 1.7 m and a length of 1.4 m.

In order to achieve the required magnetic field, the coil cross-sections will have to have a current density in range of 100 to 140 A/mm^2. The magnet is designed to provide an open bore diameter of 0.9 m over a length of 1.4 m. The magnet will be operating at 60% of the critical current of the conductor used. The magnet coils will be wound over an aluminium AA5083 alloy bobbin which will be mechanically fixed on to the inner helium vessel made of SS 304L to prevent any movement during the operation. The magnet is designed to be symmetric around the central axis (z-axis) and also across x-y plane. Thus the coils form four symmetrical pairs, i.e. coils (1, 2), (3, 4), (5, 6) and (7, 8) as indicated in Fig. 1. The magnet and the Helium vessel will be supported by support rods which ensure that there is no variation to the magnet axis.

3 Methodology

The magnet is modelled as a 2D axisymmetric case in order to reduce the computational time. In order to make such a model, effective material properties were assumed for parts where the body is periodic but not axisymmetric. Here an effective Young's modulus (*E**) can be esitmated using mixture rules where instead of a matrix and inclusion a matrix and void is considred. The effective Young's modulus is esimated as per Eq. (1) where v is the ratio of body volume of a periodc case to an axisymmetric case and E is the Young's modulus of the material.

$$E^{*} = E \times v \qquad \ldots (1)$$

Also, a symmetric condition was considered along the centre plane since the magnet is under free contraction towards the centre. The bobbin material is AA 5083 while the helium vessel bore is made of SS304L. The coil material is taken to be a combination of copper and Nb-Ti. The ratio Cu/Nb-Ti varies from 9:1 to 12:1 depending on the wire used in each coil. The PET insulation is negleted in the calcualtion since the strength and other mechanical properties are dominated by the copper and supercondutor. Based upon the composition of each coil, the effective material peoperties are calculated for each coil. The mechanical/thermal property parameters of all the constituent materials are taken from the NIST database over –the whole temperature range of 300 K to 4.2 K.[4]

The structural and thermal FEA simulation was performed in ANSYS Workbench (V18). The calacuation of Elecromagnetics is done in Dassault OPERA (V19). The whole body was meshed primarily using quad mesh. The model has an element quality from 0.471 to 0.999 with an overall average of 0.792. The mesh has an overall orthogonal quality of 0.996. The meshed axisymmetric model is shown in Fig. 2. In order to simulate the actual conditions during cooldown, sliding contact is provided between the coils and the bobbin. A frictional condition with separation is considered between the inner radius of the coil and the mating surface of bobbin. Similarly, a sliding condition without separation is considered between the bobbin and the helium vessel. Appropriate values of coefficenet of friction is assumed where ever a sliding contact condition is applied.[5] The helium vessel is in close contact with the bobbin and will restrict the radial contraction of the bobbin and the coils where the vessel is in contact with the bobbin.

4 Results

4.1 Thermal stress

The stresses and the displacement of the coils are calculated from the simulation results. Since the magnet is free to contract, the level of stress is low. This will however create a displacement of the coils from

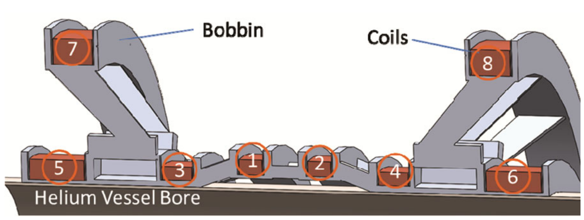

Fig. 1 — The 3D model of the 1.5T MRI magnet. The coils C1-C8 are wound in respective slots in the magnet bobbin. The whole magnet is slid over the helium vessel bore tube.

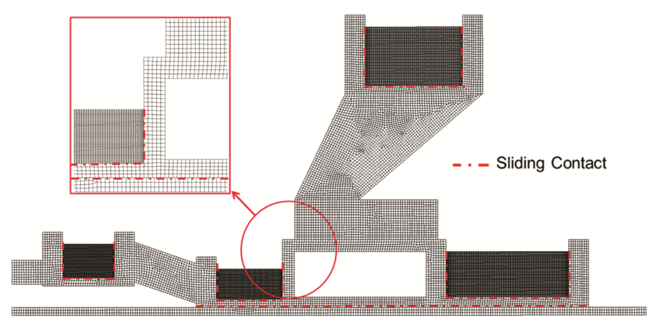

Fig. 2 — The meshed axisymmetric model of the 1.5 T MRI magnet consisting of the coils, bobbin and the He vessel bore. The contact regions where sliding condition is placed are also shown.

their original positions. Fig. 3 shows the calculated von Mises stress, along with the displacement of the coil and the bobbin. The graphs are plotted along median lines of each coil passing from the inner radius of the bobbin to the outer radius of the coil. In the bobbin, the maximum stress is in the range of 70 MPa with a few areas with stress concentration ranging up to 125 MPa. The material AA5083 – H32 used for bobbin fabrication has a 0.2% proof stress of 176 MPa and a tensile strength of 419 MPa.[6] The maximum von Mises stresses in the coils are 20.7 MPa in coils (C1, C2), 31.1 MPa in coils (C3, C4), 31.3 MPa in coils (C5, C6) and 16.7 MPa in coils (C7, C8). The 0.2% Proof Stress for the conductor used, as per test results, is >138 MPa. The calculated stresses are well within the allowable limits for the respective materials.

Considering the displacement of the bobbin and consequently the coils they are expected to move inwards both radially and axial due to thermal contraction. The thermal contraction coefficient of the bobbin material (AA 5083) is higher than Coil (Copper). This differential contraction will create a gap between the coil and bobbin in the cold condition. Further the self-contraction of coil will reduce the cross-section area changing the current density. If we examine the displacements of the bobbin and the coil, a gap can be seen between the bobbin and the coils. The gap is evident from a sudden jump of the displacement curves at the bobbin-coil interface. Considering each coil, the calculated gaps are 400 µm, 123 µm, 92 µm, 589 µm for C1, C3, C5, C7 respectively. It may be observed that the coils which are in contact with the SS304L Helium Vessel Bore have less radial movement since the bore provides extra resistance against contraction. In real life conditions, due of gravity, the coils will move downwards on to the bobbin due to the gap, creating relative movement between the coils and moves the magnetic iso-centre away from the geometric centre. These conditions together will degrade the magnetic field quality of the magnet. One of the methods employed to compensate for this relative movement is adjusting the winding tension of the coils. The winding tension thus radially pushes the coil on to the bobbin ensuring there is no gap generated.

4.2 Field Homogeneity

The relative displacements of the coils disturb the accurately designed magnetic coordinates, adversely affecting the performance of the magnet. The thermal contraction also reduces the coil cross-section. Since

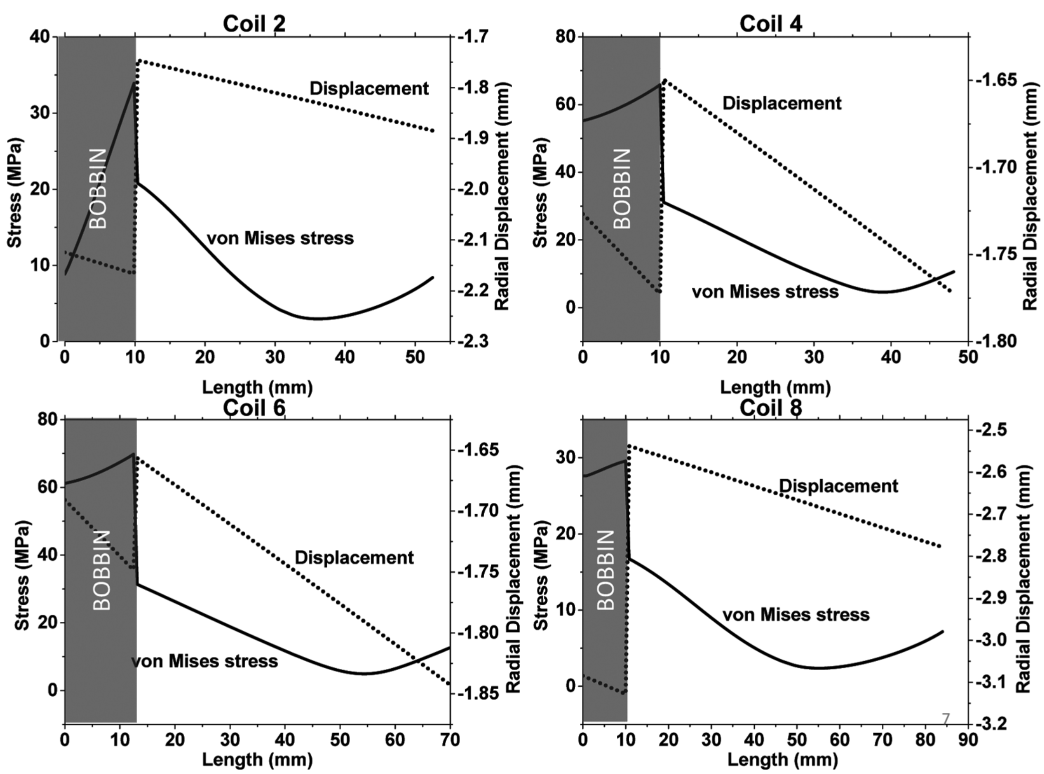

Fig. 3 — The von Mises stress and the displacement in each coil. The graphs are plotted along a median line of each coil passing from the inner radius of the bobbin to the outer radius of the coil.

the magnet operates at a fixed current, the reduction in cross-sectional area increases the current density in each coil, which in turn increases the magnetic field. One can assess adverse effects of thermal contraction by comparing the central magnetic field and the field homogeneity in the FOV before and after the thermal contraction. The Electro-Magnetic calculations of the original magnetic coordinates and the disturbed coordinates show that the central magnetic field increases from 1.499964 T to 1.505933 T. The increase in magnetic field shifts the resonance frequency of the MRI scanner to 64.122 MHz from 63.868 MHz. Plotting the variation of magnetic field within the FOV, it is found that the field homogeneity changed from 5.5 ppm to 278 ppm (Fig. 4). The gap formed during contraction, will also cause downward movement of coils. This movement destroys the symmetry of the magnetic field across the horizontal axis of the FOV.

The axial magnetic field inside the FOV can also be expressed in terms of Legendre polynomials in Eq. (2)

$$B_z = \sum_{n=0}^{\infty} \sum_{m=0}^{n} P_n^m \cos\theta \; (A_n^m \cos m\emptyset + B_n^m \sin m\emptyset) \quad \ldots (2)$$

where A_n^m and B_n^m are Legendre coefficients, P_n is Legendre polynomial of the n-th order.[7,8] The zeroth order term is the central field and higher order terms are the harmonics which signify in homogeneity of the magnetic field. It may be noted that for coil pairs symmetric about a plane, odd order terms are zero ($A_n^0 = 0$ and $B_n^0 = 0$ when n is odd).[9] It is found that the cool down of the magnet and the resultant relative displacements introduce new harmonic terms, mostly in 2nd and 3rd order terms, which were not present before the cooldown. Table 1 shows the coefficients of Legendre polynomials up to 16th order before and

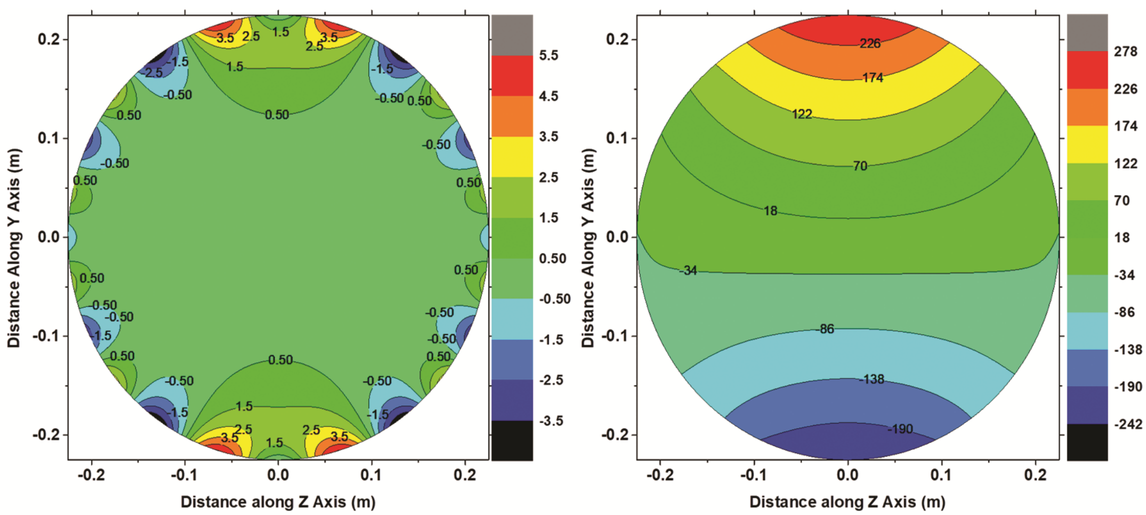

Fig. 4 — The field homogeneity (ppm) before and after the cooldown in the 45 cm FOV at the iso-center of the magnet. The homogeneity changed from 5.5 ppm to 278 ppm due to relative movement of coils due to cooldown.

Table 1 — The Legendre coefficients of the axial field in the FOV before and after cooldown. New terms were introduced to the series due to distortions produced by the cooldown.

Order		Before Cooldown		After Cooldown	
n	m	A_n^m	B_n^m	A_n^m	B_n^m
0	0	1.499964	0	1.505933	0
1	1	2.01E-16	1.11E-16	1.25E-16	3.15E-04
2	0	9.99E-07	0	-4.90E-05	0
2	2	-2.08E-17	-1.69E-16	-3.06E-08	-1.56E-16
3	1	-3.64E-17	8.81E-18	1.30E-16	-4.70E-05
4	0	3.73E-06	0	6.70E-06	0
5	1	-2.26E-17	-1.27E-17	7.89E-17	3.34E-06
6	0	3.16E-06	0	-3.03E-06	0
7	1	2.36E-17	-1.18E-17	4.68E-17	1.00E-07
8	0	4.43E-06	0	5.72E-06	0
9	0	-1.34E-15	0	-1.70E-15	0

after cool down. Here the 1st order harmonics can be corrected during the operation using the Gradient coils which also will be used for scanning. The 2nd order harmonic terms are corrected using dedicated coils installed in the magnet bore, called active shimming coils. 3rd order (or higher) shimming is usually available for MR systems with field strengths above 3 Tesla.[10]

Thermal stresses and strain will always be present in superconducting magnets due to cool down to very low temperatures. Few methods can be employed to manage the effects of the cool down. To reduce the gap between the bobbin and the coils, during manufacturing, the magnet is wound at a pre-calculated tension.[11] This pre-stresses the coils and keeps them pressed on to the bobbin even after cool down. The amount of winding tension is determined based on the thermal stresses discussed above. It may be noted that the winding tension also has to compensate for the Lorentz forces produced in the magnet during operation which act radially outward on every coil. The higher winding tension on the other hand increases the total stress on the coils. So, the calculation of the winding tension is about finding the optimized point while compensating between the field homogeneity of the magnet and the stress level on the winding. Another method usually taken to reduce the effect of thermal stress is at the magnet design stage such that even though the designed magnet coordinates show a very high in homogeneity but once the magnet is cooled down to 4.2 K, the distorted magnetic coordinates can provide the expected level of homogeneity. A combination of above methods along with proper shimming is used to obtain the required magnetic field and field homogeneity in an MRI scanner.

5 Conclusion

We have discussed the effect of cool down (300 K to 4.2 K) of a 1.5 T MRI magnet on its field homogeneity. The thermal stresses and corresponding movement of the coils have been estimated using numerical analysis. The maximum stress in the coils and bobbin are calculated to be 31.3 MPa and 60 MPa respectively, which are well within the allowable stress limits of the respective materials used in the magnet coils and the bobbin. The strains and the movement of the coils were also calculated and their effect presented. The central field increased from 1.499964 T to 1.505933 T increasing the resonant frequency of the system by 0.25 MHz. The magnetic field homogeneity degraded from 5.5 ppm to 278 ppm due to the movement of the coils. The field homogeneity when analyzed in terms of Legendre polynomials also shows that new higher order harmonic terms enter the magnetic field expansion equation. Few methods to manage the effects of the thermal stresses have also been discussed.

Acknowledgement

Authors would like to acknowledge the help and support of the members of IMRI project, IUAC. This work is funded by Ministry of Electronics and Information Technology, Govt. of India as part of the Indigenous Magnetic Resonance Imaging Project, SCAN-ERA.

References

1 Lvovsky Y & Jarvis P, *IEEE Trans Appl Supercond*, 15 (2005) 1317
2 Thekkethil S R, Kar S, Kumar M, Soni V, Suman N K, Sharma R G, Rastogi V & Datta T S, *IEEE Trans Appl Supercond*, 28:4 (2018) 441905
3 Kar S, Suman N, Thekkethil S R, Soni V, Kumar R, Saini SK, Sharma R G, & Datta T S, *Indian J Cryog* 44 (2019) 193.
4 https://trc.nist.gov/cryogenics/materials/materialproperties.htm (24 Aug 2022)
5 Brice H, Theiler G & Gradt T. *IEEE Trans Appl Supercond*, 22 (2012) 4400204
6 Huang C, Wu Z, Huang R, Wang W & Li L. *IOP Conf Ser Mater Sci Eng*, 279 (2017) 012002.
7 Iwasa Y, *Case Studies in Superconducting Magnets: Design and Operational Issues, 2nd ed.* (Springer New York) 1994
8 *Opera-3d User Guide 18R2* (Cobham Technical Services, UK) 2016.
9 Lvovsky Y, Stautner E W & Zhang T, S*upercond Sci Technol*, 26 (2013) 93001.
10 Blasche M & Fischer D, *Magnet Homogeneity and Shimming,* (Siemens Healthcare, Germany) 2015
11 Thekkethil S R, Kar S, Suman N, Kumar M, Soni V, Sharma R G, & Datta T S, *Indian J Cryog*, 43 (2018) 187